

# Verification of TMI-adjusted rainfall analyses of tropical cyclones at ECMWF using TRMM Precipitation Radar observations

Angela Benedetti, Philippe Lopez,  
Emmanuel Moreau and Peter Bauer

Research Department

To be submitted to *Journal of Applied Meteorology*

October 2004

*This paper has not been published and should be regarded as an Internal Report from ECMWF.  
Permission to quote from it should be obtained from the ECMWF.*



European Centre for Medium-Range Weather Forecasts  
Europäisches Zentrum für mittelfristige Wettervorhersage  
Centre européen pour les prévisions météorologiques à moyen terme

Series: ECMWF Technical Memoranda

A full list of ECMWF Publications can be found on our web site under:

<http://www.ecmwf.int/publications/>

Contact: library@ecmwf.int

©Copyright 2004

European Centre for Medium-Range Weather Forecasts  
Shinfield Park, Reading, RG2 9AX, England

Literary and scientific copyrights belong to ECMWF and are reserved in all countries. This publication is not to be reprinted or translated in whole or in part without the written permission of the Director. Appropriate non-commercial use will normally be granted under the condition that reference is made to ECMWF.

The information within this publication is given in good faith and considered to be true, but ECMWF accepts no liability for error, omission and for loss or damage arising from its use.



## Abstract

A validation of passive microwave-adjusted rainfall analyses of tropical cyclones using spaceborne radar data is presented. This effort is part of the 1D+4D-Var rain assimilation project which is being carried out at the European Centre for Medium-Range Weather Forecasts (ECMWF). Brightness temperatures or surface rainrates from the Tropical Rainfall Measuring Mission (TRMM) satellite are processed through a 1D-Var retrieval to derive values of Total Column Water Vapor (TCWV) which can be ingested into the operational ECMWF 4D-Var. As an indirect validation, the precipitation fields produced at the end of the 1D-Var minimization process are converted into *equivalent radar reflectivity* at the frequency of the TRMM Precipitation Radar (13.8 GHz) and compared to the observations averaged at model resolution. The averaging process is validated using a sophisticated downscaling/upscaling approach which is based on wavelet decomposition. The Precipitation Radar measurements are ideal for this validation exercise, being perfectly co-located but completely independent of the TRMM Microwave Radiometer measurements. Qualitative and statistical comparisons between radar observations and retrievals from the TMI-derived surface rainrates and from TMI radiances, are carried out using seventeen well-documented tropical cyclone occurrences between January and April 2003. Several statistical measures such as bias, root mean square error and Heidke Skill Score are introduced to assess the 1D-Var skill as well as the model background skill in producing a realistic rain distribution. Results show a good degree of skill in the retrievals, especially near the surface and for medium-heavy rain. The model background appears to produce enough precipitation in the domain, sometimes in excess, and often shows an error in the location of precipitation maxima. Differences between the two 1D-Var approaches are not large enough to make final conclusions regarding the advantages of one method over the other. While both methods are capable of redistributing the rain patterns according to the observations it appears, however, that the brightness temperature approach is in general more effective in increasing precipitation amounts.

## 1. Introduction

Tropical rainfall is a key component of the hydrological cycle and largely influences the global energy exchange ([Webster, 1994](#)), yet numerical models often fail to represent it realistically, particularly at the spatial scales typical of tropical cyclones and hurricanes ([Le Marshall et al., 2002](#)). An assessment of the quality of the precipitation analyses for these weather occurrences is important to understand strengths and deficiencies of current forecast/assimilation systems, also in view of future weather/climate projections. Particularly suited to evaluate model skills in precipitation analysis in the Tropics are the observations made available from the Tropical Rainfall Measuring Mission (TRMM) satellite ([Simpson et al., 1996](#)). TRMM has so far provided reliable and accurate rainfall observations from complementary instruments such as the TRMM Microwave Imager (TMI), the Visible and Infrared Scanner (VIIRS), the Lightning Imaging Sensor (LIS) and the Precipitation Radar (PR). The latter, in particular, offers a unique three-dimensional view of precipitating clouds at high spatial resolution ([Kozu et al., 2001](#)) and is used in this study to investigate the quality of the ECMWF 1D-Var precipitation analyses of tropical cyclones.

Since 1998, there has been an ongoing effort to assimilate retrieved rainrates from the TMI and SSM/I instruments into the ECMWF model. [Marécal and Mahfouf \(2000\)](#) pioneered work in that direction by using TMI and SSM/I surface rain rates to correct the model first guess (background<sup>1</sup>) in a one-dimensional variational context. Their results showed that the initial model precipitation field could be improved by including observations; however, when the same observations were used directly in the full ECMWF 4D-Var assimilation system, in some cases convergence to the optimal solution was not attainable. Hence they devised a 1D+4D-Var approach in which the TMI or SSM/I surface rainrates are processed within the 1D-Var system and the corresponding increments in specific humidity are converted into pseudo-observations of TCWV that can be easily ingested in the incremental 4D-Var system ([Courtier et al., 1994](#)). Their work has been continued

<sup>1</sup>From this point on the two terms are going to be used interchangeably.

and extended to the 1D–Var and 1D+4D–Var assimilation of brightness temperatures via the use of a radiative transfer operator and its adjoint by [Bauer \(2002\)](#) and [Moreau et al. \(2004\)](#). [Moreau et al. \(2004\)](#) (hereafter M04) compare the direct use of brightness temperatures versus the use of pre-retrieved surface rainfall rates. Some of the advantages of using brightness temperatures include a direct control of the assumptions that go into the conversion of the model state variables into microwave brightness temperatures via the use of a Radiative Transfer Model. The direct use of brightness temperatures also ensures a greater flexibility in selecting useful channels and in defining observational errors. These advantages come at the expense of a higher computational speed than that of the surface rainfall-based retrievals. Although interesting in their own right, these criteria might not be objective enough to solve the dilemma of the use of derived products versus the use of direct measurements into assimilation systems. As a follow-up to M04, this study aims at providing tools to quantify the benefits of one method with respect to the other by using observations from the TRMM/PR, which are independent of the TMI measurements but perfectly co-located. A by-product of this assessment is the quantitative evaluation of the forecast model skills in rainfall prediction as well as the quantification of the possible benefits of rainfall assimilation toward improving that prediction. The focus is mainly on tropical cyclones but some of the findings discussed in this article have a more general applicability.

The road map of the paper is as follows. Section [2](#). briefly introduces the 1D–Var technique used at ECMWF to assimilate rain information from the TMI measurements. The approach to derive radar reflectivities at 13.8 GHz (TRMM–PR frequency) from ECMWF three-dimensional model fields is also briefly presented. A discussion of the representativeness issues involved in the comparison of model fields and observations which have different resolutions is presented in section [3](#). along with a new application of a statistical upscaling technique to validate the PR averages. A description of the methods used for the evaluation of the ECMWF 1D–Var/TMI retrievals is presented in section [4](#). and [5](#). along with an overview of results using seventeen occurrences of tropical cyclones between January and April 2003. Summary and conclusions are outlined in section [6](#).

## 2. General overview

In this study, the results of the 1D–Var/TRMM retrievals presented in M04 are examined and compared with observations from the Precipitation Radar. A general presentation of these 1D–Var retrievals and of the forward reflectivity model is provided below.

### a. 1D–Var retrievals

Given an atmospheric background state of temperature, specific humidity and surface pressure ( $\mathbf{x}_b$ ), and a forward model ( $F$ ) that relates the model state ( $\mathbf{x}$ ) to a set of observations ( $\mathbf{y}$ ), it is possible to solve the inverse problem in a variational context and derive the atmospheric state for which the least-square distance between the observations and their model counterparts is at a minimum subject to an *a priori* constraint (also called background). This is obtained by optimizing the following functional

$$J = \frac{1}{2}(\mathbf{x} - \mathbf{x}_b)^T \mathbf{B}^{-1} (\mathbf{x} - \mathbf{x}_b) + \frac{1}{2}(F(\mathbf{x}) - \mathbf{y})^T \mathbf{R}^{-1} (F(\mathbf{x}) - \mathbf{y}) \quad (1)$$

where  $\mathbf{B}$  represents the background error covariance matrix and  $\mathbf{R}$  represents the observation error covariance matrix which includes both instrumental errors and forward model errors. The operator  $F$  allows to go from model space to observational space and is defined according to the type of observations of interest. For example for the 1D–Var which makes use of TMI surface rainfall rates derived from the PATER algorithm ([Bauer and Schluessel, 1993](#); [Bauer et al., 2001](#)) (hereafter 1D/RR), the forward model consists of the moist



physics schemes that describe the large-scale condensation ([Tompkins and Janisková, 2004](#)) and the convection ([Lopez and Moreau, 2004](#)). For the 1D–Var which makes use of TMI brightness temperatures (hereafter 1D/TB), the forward model consists of the same physical parameterizations plus a Radiative Transfer Model (RTM) that takes into account the scattering and absorption of microwave radiation in precipitating clouds ([Bauer, 2002](#); [Moreau et al., 2002](#)).

The initial atmospheric state which is also used as the background throughout the minimization is provided by 12-hour T511 integrations of the ECMWF model. Input fields include the vertical profiles of temperature and water vapor as well as temperature and humidity tendencies, surface heat fluxes and surface momentum stress that are needed in the convection scheme. For the 1D/TB, additional inputs such as the 2-meter temperature and the 10-meter winds are required in order to run the RTM. More details on the implementation of the 1D–Var with TMI surface rainfall rates and brightness temperatures are provided in M04.

The direct outputs of the 1D–Var are the “optimal” temperature and specific humidity profiles; from these variables it is possible to derive precipitation and cloud amounts by running again the physical schemes. In the next section we describe the approach used here to compute the equivalent radar reflectivity from the 1D–Var outputs.

#### *b. Reflectivity forward model*

The radar backscattering cross-section derived from the radar return power can be related to the amount of solid precipitation (rain and snow) and the amount of cloud ice/water content that the radar signal encounters in its path. The forward modeling of this radar signal can be performed by assuming a size distribution of the scatterers and by computing their optical properties. Here it is assumed that all rain/snow/cloud ice and water particles are spherical. Their optical properties are computed using the Mie solution at the frequency of interest (13.8 GHz for the TRMM/PR) and as functions of temperature, and then integrated by assuming a Marshall–Palmer distribution for the precipitation-sized particles ([Marshall and Palmer, 1948](#)) and a modified–gamma distribution for the cloud particles ([Stephens et al., 1990](#)). The radar reflectivity factor is proportional to the integral of the backscattering cross–section over the size distribution. A variable commonly used to describe the radar return is the equivalent radar reflectivity, hereafter indicated with the symbol Z, which represents the radar reflectivity factor that would be associated with an equivalent volume of spherical water droplets. If the target particles are in a solid phase, it is necessary to convert the raw reflectivity factor into an equivalent reflectivity. This is done in the forward model assuming a fixed density for the snow ( $\rho=0.1 \text{ g cm}^{-3}$ ) and cloud ice particles ( $\rho=0.9 \text{ g cm}^{-3}$ ).

In the presence of intense precipitation, the radar signal is attenuated. By computing the total optical depth and the path–integrated attenuation, the attenuated profile of reflectivity can be recovered. Here, however, we make use of the unattenuated reflectivity product from the TRMM 2A25 algorithm ([Iguchi et al., 2000](#)) and hence we do not take attenuation into account in the forward modeling of reflectivity, although the radar forward model has that capability. To speed up computational time, all reflectivity values computed with this forward model are collected in a look–up table and organized according to the values of temperature and cloud water and precipitation contents, which are direct outputs of the ECMWF model. A bilinear interpolation is then applied to extract the reflectivity value corresponding to the given temperature and hydrometeor contents. A special treatment of the melting layer ([Bauer, 2001](#)) is also included in the computation of the look–up table, although it is only applied at exactly 0°C. The reflectivity values contained in the look–up table were verified against those derived from other forward models and those derived from simple Z–R relationship. Comparisons show that the current forward model is reliable within a few dBZs. Research to quantify forward modeling errors is ongoing.

i. *Sensitivity to snow fall velocity assumptions.* The ECMWF model has four standard hydrometeor categories: prognostic cloud ice/water and diagnostic rain and snow. Cloud particles are assumed to fall at a fixed velocity parameterized as a function of the water content. Rain and snow are assumed to reach the ground in one time step. For the treatment of these hydrometeors in the forward reflectivity code, it is necessary to derive a rain/snow content profile from the precipitation fluxes. By assuming a fall velocity–diameter relationship and by integrating over the Marshall–Palmer distribution it is possible to relate the precipitation fluxes directly to the rain/snow contents via a power–law relationship of the form

$$R = \sigma(WC)^\delta, \quad (2)$$

where  $R$  is the rainfall rate in  $\text{mmh}^{-1}$  and  $WC$  is the Rain Water Content in  $\text{gm}^{-3}$ . For rain we used  $\delta= 20.95$  and  $\sigma=1.12$ .

While admittedly there are uncertainties in fall speed relationships for raindrops, even larger uncertainties exist for snow particles due to the complicated crystal and aggregates geometries. Acknowledging this problem, we tested various fall speed assumptions for the snow particles using the empirical coefficients provided in [Locatelli and Hobbs \(1974\)](#) for snow categories ranging from aggregates to graupel. After some trials, it was decided to adopt the lump graupel category from [Locatelli and Hobbs \(1974\)](#), for which the modeled reflectivity had the closest resemblance to the observations in terms of melting layer height and reflectivity magnitudes. For this category the implied  $\delta$  and  $\sigma$  parameters are 5.9 and 1.12, respectively. However, the question of the optimal parameters for the fall speed velocity is still open, and improved observations would be helpful in narrowing down the uncertainties on these parameters.

#### c. PR characteristics

A detailed overview of the specifications of the TRMM Precipitation Radar is presented in [Kozu et al. \(2001\)](#). Here we report some general characteristics that can be helpful to understand the type of rain/snowfall observations that are obtained with a spaceborne active sensor.

The PR is a scanning radar which operates at 13.8 GHz; the cross–track scanning swath is 215 km and the cross–range spatial resolution is about 4.3 km. The vertical resolution is about 250 m. The minimum detectable signal is 0.7  $\text{mmh}^{-1}$  which corresponds approximately to 17 dBZ when using [Kozu et al.](#)'s effective reflectivity–rainfall rate conversion ( $Z = 372R^{1.54}$ ,  $Z$  in  $\text{mm}^6\text{m}^{-3}$  and  $R$  in  $\text{mmh}^{-1}$ ).

The benefits of space–based radar observations include, amongst others, estimates of precipitation profiles which are independent of the background surface (land or ocean); information on the vertical storm structure which, in turn, is important for the estimation of the diabatic heating profile; and a high spatial resolution that offers a view of the storm rainfall characteristics which is complementary to the passive microwave measurements and which can be used to improve the quality of the passive microwave retrievals (i.e., PATER, [Bauer et al. \(2001\)](#)). These characteristics also make the PR measurements useful for the validation of atmospheric models in terms of rain intensity and location. Shortcomings to this application are, however, the limited spatial coverage and the low observational repetition rate over the same area of the globe. In the next section we will discuss other issues that are likely to be encountered when using this type of observations for the evaluation of global model fields.

## 3. Methodology

Large–scale models such as the ECMWF model are formulated in terms of average values within the grid cell. Although some amount of subgrid–scale variability is accounted for in some models (for example in the



ECMWF forecasting system there are prognostic equations for fractional cloud cover), the output fields are nonetheless grid-average values. Because of the non-uniform distribution of moist fields, neglecting their spatial sub-grid variability may cause errors in the calculation of key parameters such as radiative fluxes and affects the model prediction ([Pincus and Klein, 2001](#)). If these model fields are then used in rainfall retrievals, the error can propagate to the retrieved rain rates and introduce regional or storm-dependent biases ([Harris and Foufoula-Georgiou, 2001](#); [Harris et al., 2003](#)).

When using high-resolution observations to evaluate coarser-resolution model fields, a question that arises naturally is that of matching the spatial scale between model and observations for a fair comparison. Errors deriving from scale mismatch, also known as “representativeness errors”, are not related to errors in the physics. However they may constitute a large portion of the model error, hence masking errors likely coming from the unresolved physics or from specific model parameterizations ([Tustison et al., 2001](#)). In order to address this issue some research efforts have been directed to downscaling large-scale model fields using statistical models parameterized in terms of physical quantities ([Perica and Foufoula-Georgiou, 1996a,b](#)); while others have looked at a combination of upscaling (averaging) and downscaling techniques ([Tustison et al., 2003](#)). In this paper, the upscaling perspective is discussed in detail.

The upscaling problem is, in a way, similar to the non-uniform beam filling (NUBF) for spaceborne instruments. When observing from space a rain field which is not uniform over the scale of the instrument horizontal range, there is the risk of introducing a bias in the estimation of the rain fall amount if the assumption of uniform distribution is used. Although this problem is more relevant for passive instruments, such as the TMI or SSM/I which have larger Field Of View (FOV), it has been of concern in the development of rainfall retrieval algorithms for the PR as discussed in [Kozu and Iguchi \(2001\)](#) and [Iguchi et al. \(2000\)](#). In those studies, the focus is to compute a correction to the coefficients of the Z-R relationship which accounts for the NUBF by assuming a predefined distribution of rain within the radar footprint. Depending on the assumption regarding the rain distribution, different values for the correction are obtained. In 2A25, the rain is assumed to be distributed according to a log-normal distribution.

#### *a. Upscaling PR data at model resolution*

The operational forecast model is currently run with 60 vertical levels in the T511 configuration which corresponds to a horizontal resolution of roughly 40 km at the Equator. As mentioned previously, the PR footprint at the Earth's surface is 4.3 km which implies that approximately one hundred radar pixels are comprised in a horizontal slice of the model grid box when the radar swath fully overlaps with one cell of the ECMWF grid. The approach taken here is to count the number of PR points in the model cell and then compute the linear average in reflectivity space. This method has the intrinsic flaw of weighting all the reflectivity values in the same way, hence implying that the sub-grid distribution of the reflectivity is uniform over the model grid box, an assumption which is not always satisfied, especially at the edges of the cyclone. Another possible approach is to assume that the rain is uniformly distributed within the model cell and compute the implied distribution for the radar reflectivity by assuming that  $Z$  and  $R$  are related through a power-law. This second approach presents some problems due to the dependence of the PDF on the assumed power-law coefficients. Moreover, the assumption of uniformly-distributed rain is not often satisfied. A third approach involves the definition of an empirical probability distribution function (PDF) based on the PR observations aggregated at the ECMWF model resolution. An attempt at using this technique was frustrated by the realization that the empirical PDF was biasing the estimates of the averages, especially for “atypical” storms. This was probably due to the fact that the intrinsic variability of the rain distribution cannot be well characterized in terms of only one PDF. After much consideration, it was hence decided to use a simple average (uniform PDF) which has the advantage of being the least biased, especially when the number of PR points over the model grid is sufficiently large.

A statistical downscaling/upscaling technique developed by [Perica and Foufoula-Georgiou \(1996a\)](#) (hereafter, PF96a) and based on wavelet decomposition was used to validate the averages of the PR reflectivities for the tropical cyclones listed in table 1. The downscaling software was kindly provided by V. Venugopal of Uni-

*Table 1: List of tropical cyclones used for the statistical validation. Indicated time refers to overpass over the Equator.*

No.	Name	Date	Time (UTC)	Latitude (deg)	Longitude (deg)
1	AMI	13-01-03	02:59	27.5S-11.7S	174.9E-172.9W
2	AMI	14-01-03	19:33	31S-20.1S	178.4W-167.0W
3	CILLA	27-01-03	12:22	25.5S-14.0S	178.4E-167.7W
4	BENI	28-01-03	19:59	24.7S-8.9S	156.0E-173.5E
5	HAPE	12-02-03	20:52	26.7S-10.4S	52.2E-73.1E
6	HAPE	12-02-03	11:45	22.1S-10.0S	60.7E-74.6E
7	GERRY	13-02-03	12:27	28.9S-14.4S	53.5E-68.7E
8	GERRY	14-02-03	18:05	32.9S-19.6S	57.5E-72.9E
9	GERRY	15-02-03	12:15	34.7S-21.9S	60.4E-71.8E
10	JAPHET	27-02-03	14:06	28.0S-17.0S	32.9E-48.8E
11	JAPHET	28-02-03	06:37	28.3S-18.0S	32.4E-42.9E
12	KALUNDE	7-03-03	23:20	22.7S-8.5S	64.7E-82.7E
13	KALUNDE	9-03-03	23:05	22.8S-11.1S	61.8E-72.9E
14	KALUNDE	12-03-03	21:56	25.4S-13.8S	59.1E-70.1E
15	KALUNDE	14-03-03	21:44	31.7S-19.8S	60.5E-73.0E
16	KUJIRA	16-04-03	11:05	8.4N-19.1N	129.3E-141.1E
17	KUJIRA	17-04-03	19:59	6.9N-18.6N	122.9E-138.2E

versity of Minnesota. In a way, this represents an “inverse” application of the downscaling method. These statistical models are in fact used to enhance model resolution, i.e. create a statistical representation of model fields at much finer resolutions than those the original large-scale model is able to resolve. In this study, however, it was chosen to use the statistical approach to verify the upscaled fields off-line. The implicit assumption is that the statistical upscaling is able to provide a better representation of the coarse-resolution field than the raw average, and hence can be used to validate it. Ultimately it would be desirable to use directly this statistical approach to compute the average itself or, even better, to use it in the “forward” direction to downscale the numerical model to the resolution of the observations. This is subject of ongoing research. For the time being however, due to the technical complexities of a full-blown implementation of the statistical downscaling model, it is only used in the “reverse” configuration. Next section briefly describes the technique and provides further references.

#### b. Statistical approach to downscaling/upscaling

All statistical downscaling models are based on the assumptions that a field at a certain scale contains information about other scales. The upscaling process, i.e. the averaging, smooths out information from the high-resolution fields and the fine-scale information is hence lost. A way to preserve this information is to find some descriptors of statistical characteristics that are scale-invariant, i.e. constant at least over a significant range of scales, and use them to reconstruct the information lost in the upscaling.

The model described in PF96a is based on two main hypotheses: (1) normalized rainfall fluctuations defined using an orthogonal Haar wavelet transform of the original rainfall field exhibit simple scaling over a range of scales, and (2) the scaling parameters can be related to thermodynamic quantities of the storm environment.



Using data from the 1985 PRE-STORM experiment (Cunning, 1986), they analyzed several radar scans providing surface rainfall rates for the mesoscale convective systems observed during that field campaign. Their analysis encompasses scales ranging from 4 km (the resolution of the radar data) up to 64 km. They found that rainfall fluctuations around the grid-box mean at a given scale  $m$ ,  $\xi_{m,i}$ , normalized by the mean value, exhibit simple scaling, i.e. they satisfy the following equation

$$\xi_{m,i} \stackrel{d}{=} (2^{m-1})^{H_i} \xi_{1,i} \quad (3)$$

where  $i = 1, 2, 3$  indicates the horizontal (x), the vertical (y) and the diagonal directions, respectively,  $H_i$  are the scaling exponents, which are also scale-invariant, and  $\stackrel{d}{=}$  stands for equality in distribution. The distribution that best represents this normalized fluctuations is the Gaussian distribution, for which equation (3) takes the simple form

$$\sigma_{m,i} = 2^{(m-1)H_i} \sigma_{1,i} \quad (4)$$

where  $\sigma_{m,i}$  are the standard deviations. The normalized fluctuations were found by the authors to be independent on the choice of Z–R relationship used to convert radar reflectivity into rainfall. Knowledge of the three spatial components (x, y, and diagonal) of the variance at the finest scale and of the exponent  $H$  (six parameters in total) permits the reconstruction of the variance at every scale and hence of the rainfall fluctuations distribution. An application of this technique for the analysis of the PR data is described in the following section.

### c. Quantification of the bias in the PR averages

The downscaling technique designed by PF96 is better applied to rainfall rate. The first step was hence to convert the near-surface radar reflectivities from the TRMM dataset into surface rainfall. Since the normalized rainfall fluctuations do not depend on the choice of Z–R relationship, the Marshall–Palmer formulation ( $Z = 200R^{1.6}$ ,  $Z$  in  $\text{mm}^6\text{m}^{-3}$  and  $R$  in  $\text{mmh}^{-1}$ ) was used for the conversion. The rainfall rates at the original instrument resolution (4.3 km) were interpolated on a regular x–y grid (which is also a requirement for the application of the downscaling software) to a resolution of 10x10 km which is considered as the smallest scale to avoid problems with noise. This discrete field was then “filtered” through the wavelet functions to produce the average and the three directional fluctuations at the next higher scale. A dyadic scale is chosen for convenience, which makes the second next higher scale equal to 40x40, approximately the current ECMWF model resolution. Figure 1 shows the distribution of the normalized rainfall fluctuations at 10x10 km and at 40x40 km for the three spatial directions and for the whole domain. The shape of the fluctuations approximates well a Gaussian distribution, even if some deviations are evident, especially in the horizontal (x) direction. This procedure is repeated until the final desired scale is reached. Once the field at 40x40 km was obtained through running the wavelet filter, we compared this average with the simple average. A mean bias and standard deviation were computed for all tropical cyclone occurrences. Results show that the simple average has almost no bias if compared to the upscaled average, except for a few cases where the cyclone variability was high.

*Table 2: Average biases and standard deviations of the simple average and model first guess/analyses with respect to the upscaled averages for the seventeen tropical cyclones. Units are  $\text{mm h}^{-1}$ .*

	Simple average	Model first guess	1D/TB	1D/RR
Bias	0.031	-0.1576	-0.1027	-0.1371
Standard deviation	0.8802	1.5401	1.1811	1.1416

These results imply that the simple averages can be used with a sufficient degree of confidence in the evaluation of the model fields. Also reported in table 2 are the values of the biases in rainfall rate for the model background

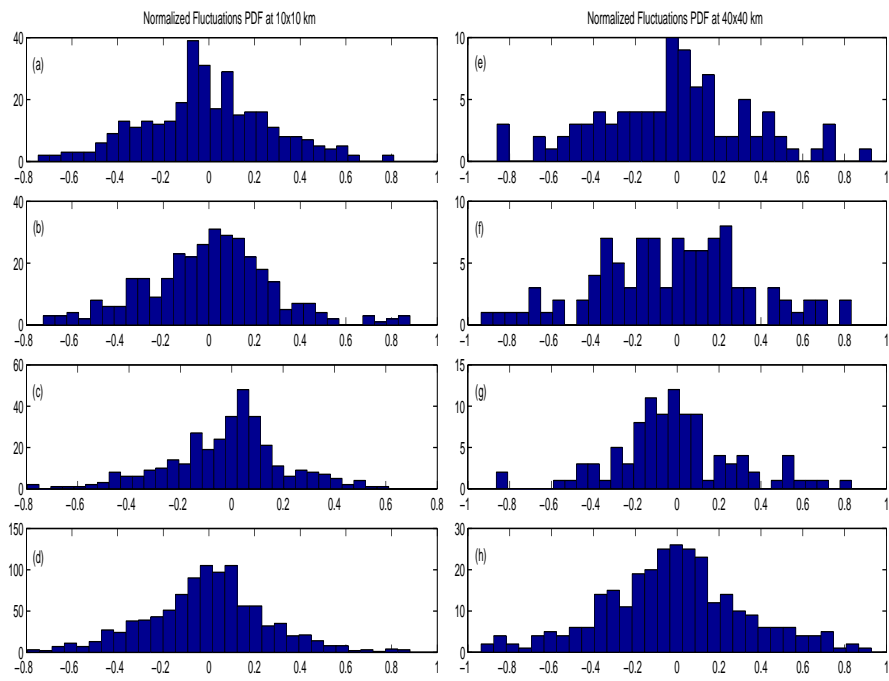


Figure 1: Sample histograms of the normalized rainfall fluctuations at 10x10 km (left column) and 40x40 km (right column): (a-e) horizontal direction; (b-f) vertical direction; (c-g) diagonal direction; (d-h) whole domain.

and the 1D–Var analyses from TMI brightness temperatures and surface rainfall rate. The difference between the upscaled average and the model fields before and after assimilation of TMI data indicates that the analysis has effectively reduced the bias.

In the following section, the PR averages verified with the procedure described above are used to assess the performance of the 1D–Var retrievals using TMI–derived rainfall rates and TMI brightness temperatures.

#### 4. Qualitative evaluation of the 1D-Var retrievals

A straightforward but qualitative method of evaluation consists in the “visual” comparison of the observed and modeled fields by means of a graphical display. While this is a quick way to establish how different/similar model and observations look, it cannot be used as an objective measure of the model performance.

More quantitative methods are based on statistical approaches where the skill of the model is measured using a set of scalar quantities. These accuracy measures are often unsatisfactory because they are not completely independent of the model configuration, but they can be useful. For a complete review of commonly used accuracy measures and their application in model verification see, e.g., Wilks (1995). For details on their use for model evaluation using non-conventional observations such as cloud water contents from radar data and optical depths from satellite sensors see, e.g., Jakob et al. (2003). Here we focus on a few commonly used model performance measures, namely the bias, the root mean-squared (rms) error, and the Heidke Skill Score. Although all these quantities can be computed for a single model forecast/analysis and the observed fields at the corresponding time, we tried to enhance our comparison by collecting a number of occurrences of tropical cyclones between January and April 2003 well observed by the TRMM instruments. Some occurrences include the same cyclone at different stages of evolution. The cyclones selected present similarities in their structure



and evolution. Most were located in the Southern Hemisphere, except for the April cases. Circa half occurred in the Indian Ocean and half in the Pacific Ocean. Names, time at satellite overpass and location of these cyclones were summarized in table 1.

As an example of qualitative evaluation we focus on cyclone AMI. Figure 2 presents a map of radar reflectivities at 2 km from (a) the PR observations linearly averaged at model resolution, (b) the model background, (c) the 1D/RR analysis and (d) the 1D/TB analysis. The units for radar reflectivities are dBZ. The background, the 1D/RR and the 1D/TB reflectivities are plotted only over the PR swath to facilitate the comparison. It appears that both 1D–Var have improved the spatial distribution and the intensity of the reflectivity field over the background, with a slightly better performance of the the 1D/TB in the central–western part of the storm. A vertical cross-section taken across the storm (25.5S-27.5S/169W-173W) is shown in figure3. The vertical structure of the storm, although improved, still shows significant differences with respect to the observed structure, mainly in terms of rainfall intensity in the heavily precipitating (high reflectivity) cells. Again the 1D/TB increases the reflectivity values bringing them closer to the PR observations.

Since radar reflectivity is strongly correlated with rainfall rate, from this preliminary assessment of model skill we can infer that the rain patterns and intensity in the model is improved by the 1D–Var assimilation either of PATER surface rainfall rates or TMI brightness temperatures. A visual analysis of the other twenty cyclone occurrences shows patterns similar to those of cyclone AMI with the background showing precipitation maxima which are wrongly located with respect to the observations, and improvements in both the 1D/RR and the 1D/TB retrievals. These improvements with respect to the background are larger than the errors in the averaged PR reflectivities; on the contrary, the differences in terms of reflectivity values amongst the two methods do not appear to be large enough to be outside the error bars of the PR averages. The statistical method should constitute a check for the qualitative results, and at same time provide a more objective way to discriminate between the two analyses.

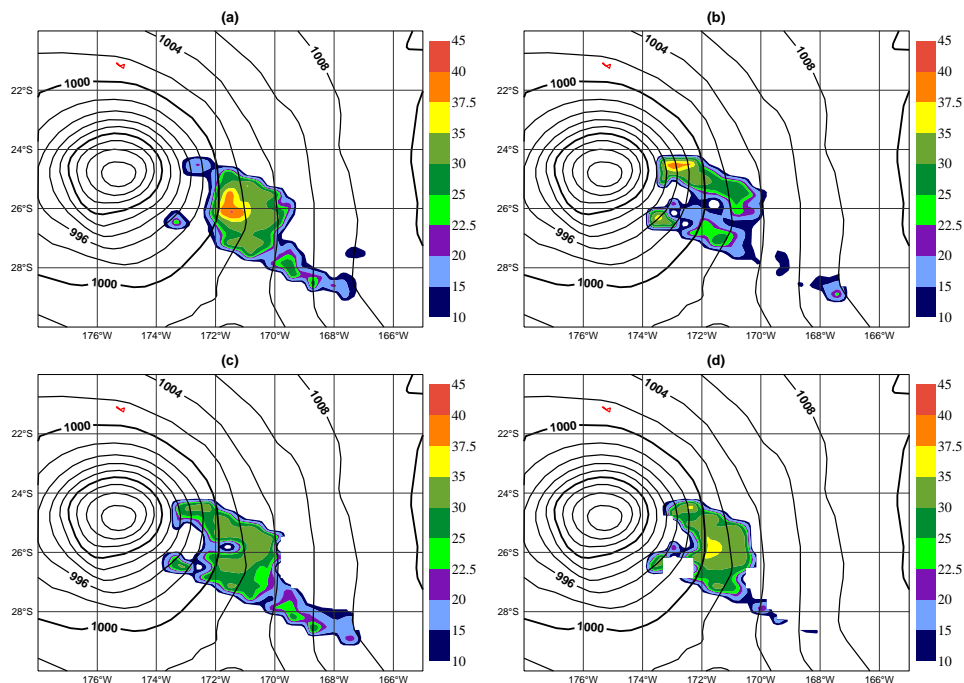


Figure 2: Maps of reflectivity fields for cyclone AMI (January 14, 2003) at 2 km derived from: (a) averaged PR observations, (b) model first guess, (c) 1D/RR and (d) 1D/TB. Units are dBZ.

## 5. Statistical evaluation

The statistical evaluation was conducted using the seventeen cases listed in table 1. All data were regrouped and processed to restrict the analysis to the points where the PR reflectivity was greater than 15 dBZ. This choice was dictated by the sensitivity threshold for the precipitation radar. Even in an average sense, the PR can only be as reliable as its sensitivity allows. Points where the 1D-Var retrievals did not converge were also excluded from the statistics. The total number of reflectivity points at 2 km after the completion of the screening was 1427.

To provide an idea of the spread in the reflectivities values, figure 4 shows a scatter-plot of the PR observations versus first guess (top), 1D/TB (center) and 1D/RR (bottom) at 2 km. The spread is considerable for all cases but appears to be reduced for the 1D-Var retrievals with respect to the background.

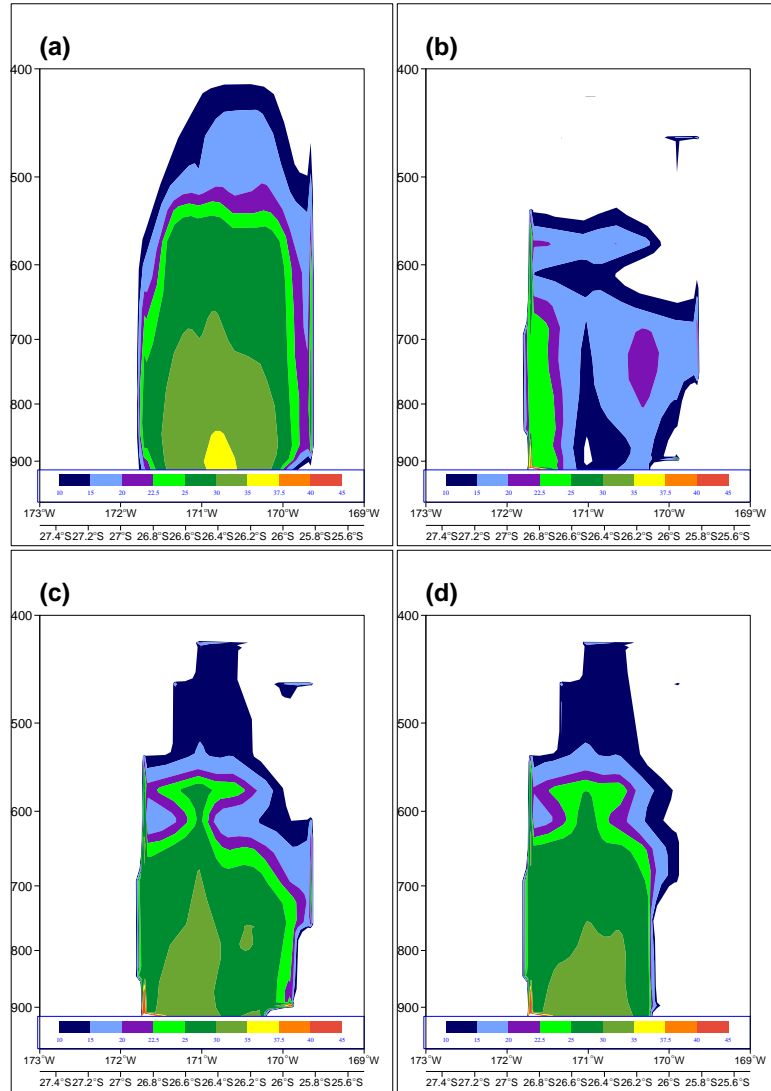


Figure 3: Maps of reflectivity fields at 2 km derived from: (a) PDF-averaged PR observations, (b) model first guess, (c) 1D/RR and (d) 1D/TB. Units are dBZ. The coordinates of the cross-section are 25.5°S–27.5°S and 169°W–173°W.

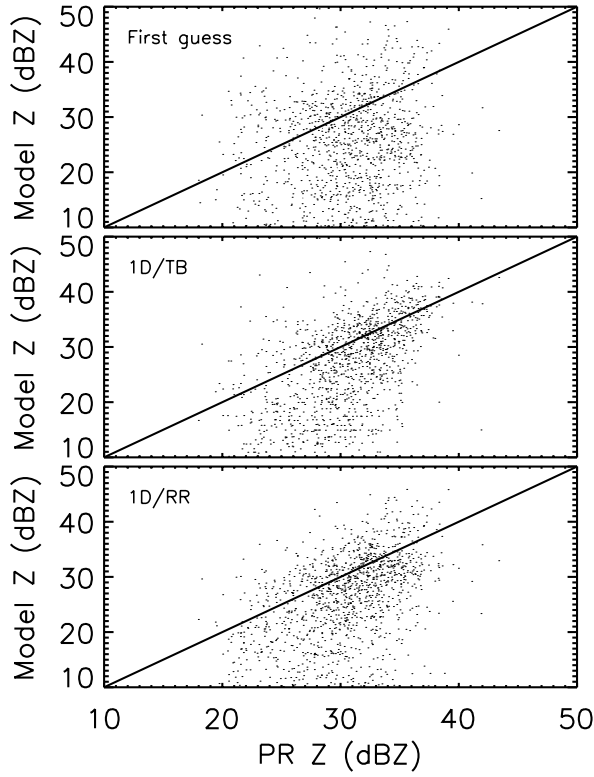


Figure 4: Scatter plot of model versus observed reflectivities for the first guess, the 1D/TB and 1D/RR.

#### a. Bias and RMS

The average model bias and the root mean square error are parameters commonly used to describe model accuracy. They operate on the gridded model and observed fields by averaging the individual differences (bias) or square differences (rms) between the two at each of the N gridpoints. To extract more information from these two parameters, we sub-divided the PR data into reflectivity bins of width 2.5 dBZ between 15 and 45 dBZ, and we computed the corresponding bias (model minus observations) and rms for each category. The results are shown in figure 5 for reflectivity data at 2 km. The thick lines represent the bias while the thin lines are the rms errors; the labelling is as follows: solid for the first guess, dashed for the 1D/RR and dotted for the 1D/TB. The shape of the bias curve is similar for all cases and shows that the model (both first guess and analyses) tend to underestimate observed reflectivities at low values and overestimate observed reflectivities at large values. However, it also shows a clear decrease between the average bias values in the first guess (around 10 dBZ) and the values for the 1D-Var retrievals (around 5 dBZ) for observed reflectivity above 20 dBZ. Concomitantly the rms errors are on average 5 dBZ higher for the first guess than for either retrieval. The performance of the two 1D-Var appears to be comparable although for reflectivities greater than 30 dBZ, the 1D/TB has a lower bias than the 1D/RR. Figure 6 shows a 2D plot of bias and rms as functions of model levels and reflectivity categories. The general trend observed in figure 5 is confirmed. Specifically, both 1D-Var perform comparably better than the first guess but differences between the two methods are smaller than the uncertainties in the PR averages. This is consistent with what was discussed in the qualitative evaluation. However, an additional consideration needs to be made regarding the slightly better performance of the 1D/TB at large reflectivity (precipitation) values. This is due to the fact that the brightness temperatures exhibit a direct sensitivity to temperature and moisture changes, hence their assimilation is more efficient in changing (in this case increasing) the precipitation intensity via the activation of the convective and large-scale condensation

Table 3: Standard 2x2 contingency table for model evaluation according to a binary classification procedure (after Conner and Petty (1998)).

	Observed YES	Observed NO
Model YES	A	C
Model NO	B	D

parameterizations. The effectiveness of the assimilation of TBs is diluted in the vertical due to the fact that the vertical structure of the temperature and specific humidity increments, hence of the precipitation, is largely determined by the background error covariance matrix.

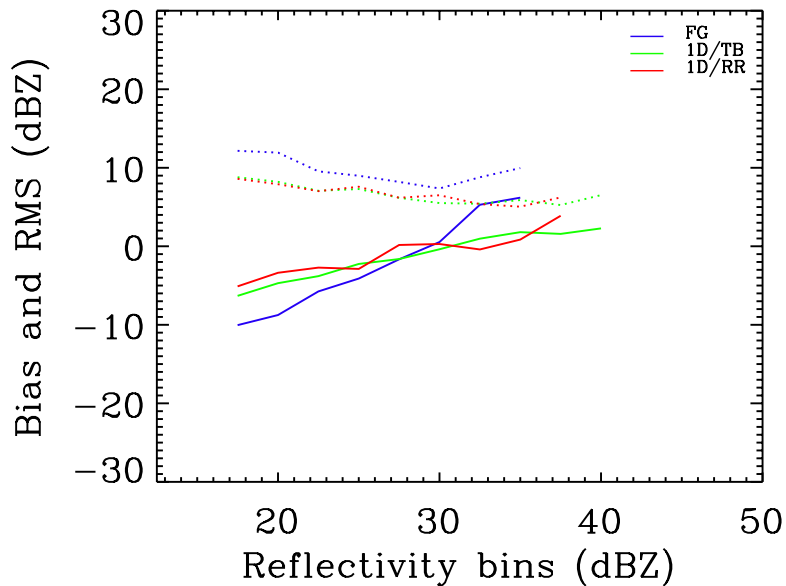


Figure 5: Bias (solid line) and rms (dotted line) with respect to PR observations for model first guess (blue), 1D/TB (green) and 1D/RR (red) for various reflectivity classes at 2km.

### b. Contingency matrix and Heidke Skill Score

The increase in skill at large reflectivity values is also illustrated by another parameter, here discussed in detail, the Heidke Skill Score (HSS). This predictor is derived from the *contingency matrix* defined in table 3 and it indicates the degree of consistency between observed and model-derived values with respect to a binary classification of a grid-point as having reflectivity greater than a certain threshold (e.g., lightly or heavily raining).

A detailed discussion of the properties of the Heidke Skill Score is provided in Conner and Petty (1998) (hereafter CP98) who also list other references related to the use of HSS and other measures of skill derived from contingency tables. The definition of HSS provided by CP98 is the following:

$$HSS = \frac{2(AD - BC)}{B^2 + C^2 + 2AD + (B+C)(A+D)} \quad (5)$$

HSS can range from -1 to 1, with 1 indicating perfect skill, 0 indicating no skill with respect to a random prediction and -1 perfect negative skill (i.e. the model has always the opposite prediction with respect to the

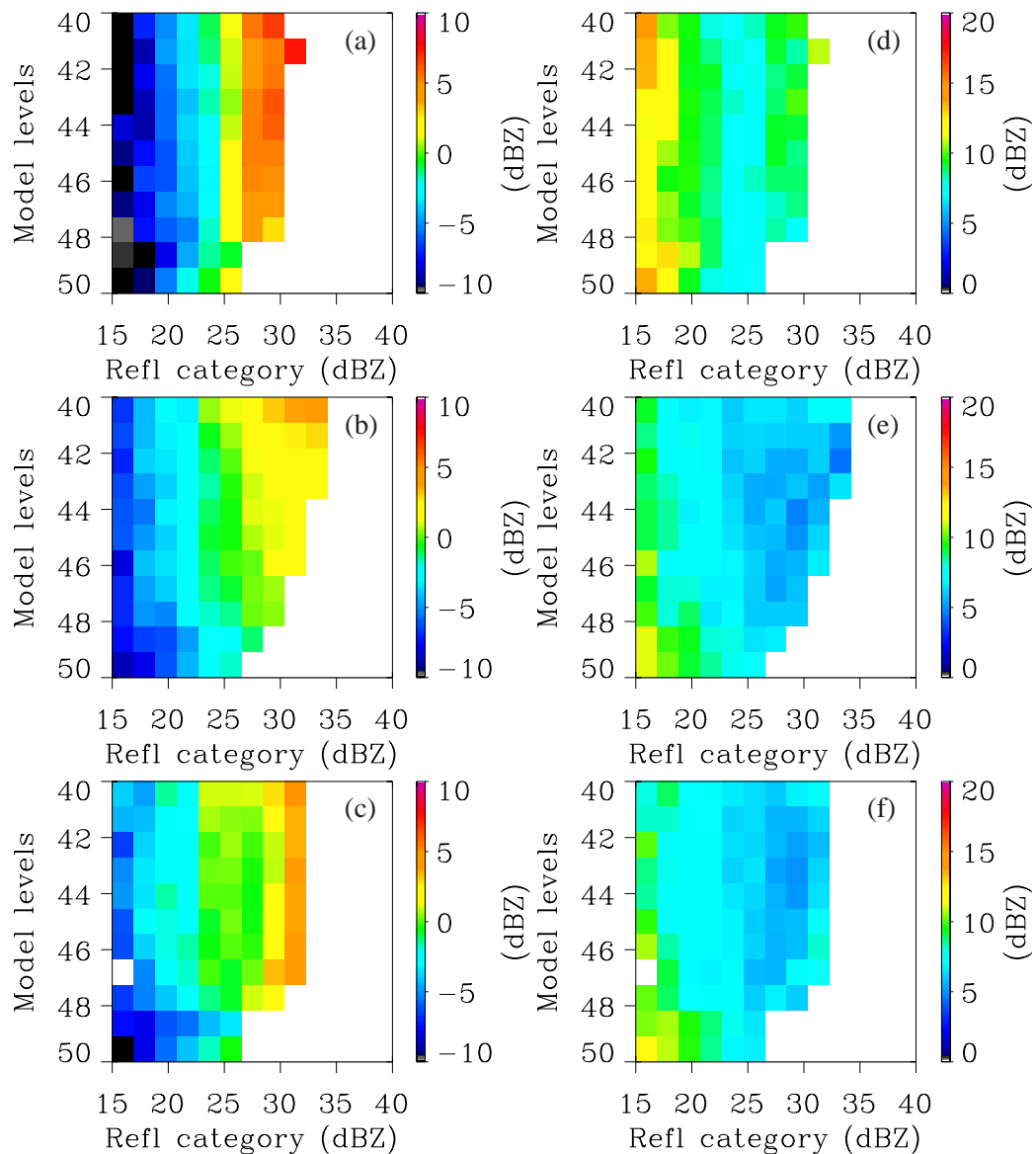


*Figure 6: Left column: vertical structure of bias (model-obs) as function of reflectivity amplitude for (a) model first guess, (b) 1D/TB and (c) 1D/RR between model level 40 and model level 50. Right column: corresponding vertical structure of rms for (d) model first guess, (e) 1D/TB and (f) 1D/RR.*

Table 4: Model skill as defined by the Heidke Skill Score for medium–heavy rain prediction ( $R > 5 \text{ mmh}^{-1}$ )

	HSS (all points)	HSS (points where PR Z > 15dBZ only)
First guess	0.130	0.129
1D/RR	0.230	0.220
1D/TB	0.323	0.414

observations). An example of application of the HSS is to determine model skill in medium–heavy precipitating events. In this case, a positive occurrence is verified when the reflectivity at 2 km is greater than 34 dBZ (which corresponds to  $R$  approximately equal to  $5 \text{ mmh}^{-1}$ , using a Marshall–Palmer Z–R conversion:  $Z = 200R^{1.6}$ ,  $Z$  in  $\text{mm}^6\text{m}^{-3}$  and  $R$  in  $\text{mmh}^{-1}$ ). In table 4 we report values of the HSS for the background forecast and the two 1D–Var analyses. The first column of values refers to a global HSS, i.e. where all the reflectivity points were included in the computation of the contingency matrix. The second column refers to an HSS computed only over the points where the PR indicated the presence of rain ( $> 0.5 \text{ mmh}^{-1}$  according to the PR sensitivity). The skill is lowest for the background and highest for 1D/TB. The fact that HSS for the first guess is larger when all points are used shows that in general the forecast produces some heavy rain in the domain, but it is not necessarily distributed as the PR observations indicate. In fact, when only the points where the PR reflectivity is greater than 15 dBZ are used, there is a small drop in the forecast skill and an increase in the 1D/TB retrieval skill. The assimilation of TMI brightness temperatures appears to have a positive impact on both the intensity and the distribution of the rain field. The 1D/RR appears to have intermediate skill in both cases. Figure 7 shows the change in model skill as measured by the Heidke Skill Score according to the choice of threshold. The plot indicates that as the reflectivity threshold increases, 1D–Var , particularly 1D/TB, is more skillful than the background.

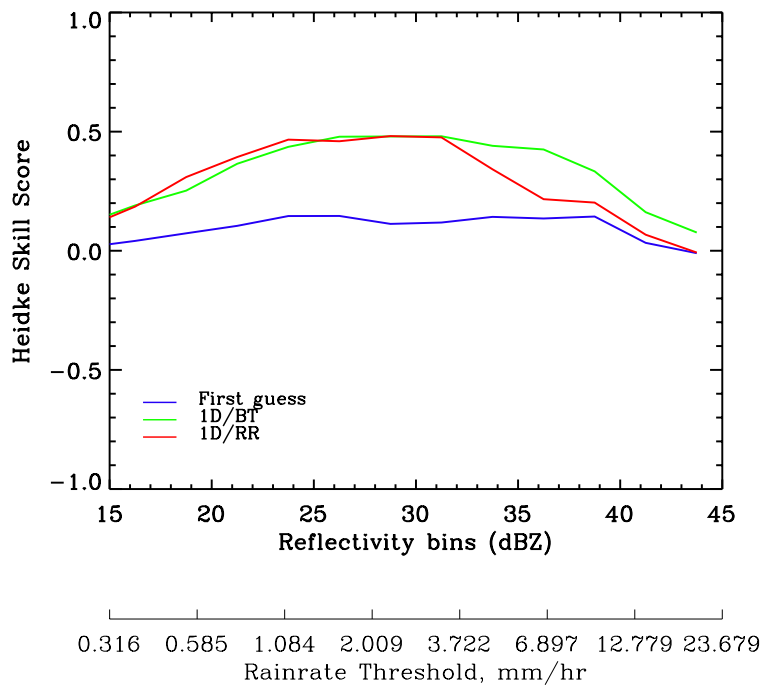


Figure 7: Heidke Skill Score as functions of reflectivity for model first guess (blue line), 1D/TB (green line) and 1D/RR (red line) (see text for explanations).



## 6. Summary and conclusions

This paper treated with some degree of detail the verification of TMI rainfall analyses performed at ECMWF using a 1D–Var approach. Two types of retrievals were discussed: the 1D/RR which makes use of *surface* rainfall rates from the PATER algorithm and the 1D/TB which makes direct use of the TMI brightness temperatures. The skill of the two retrievals relative to the skill of the model background forecast (used as first guess in the 1D–Var) was measured against independent, co-located observations from the Precipitation Radar on board of the TRMM satellite. A qualitative evaluation indicated a better skill in the 1D–Var retrievals than in the background. To enhance the evaluation, seventeen tropical cyclone occurrences were also used to derive various statistical skill indicators. Results pertaining each of these predictors (bias, rms, Heidke Skill Score) were presented and discussed. In general, all parameters confirm an improved model skill when TMI observations are used. Specifically, near the surface and for reflectivities larger than 34 dBZ (i.e. rainfall rates  $> 5 \text{ mm/h}$ ), the most promising approach for improvement appears to be 1D/TB. However, a decrease in skill is observed for all model configurations at upper levels where the model reflectivities are consistently lower with respect to their observed counterparts. From both the qualitative and the statistical analysis, no conclusion can be drawn regarding which 1D–Var method, the 1D/TB or the 1D/RR, produces rainfall analyses that are closer to the PR–observed distributions. In fact, the differences between the two methods are lower than the uncertainties associated to the PR averages.

A novel aspect of this evaluation study was the application of of statistical upscaling technique to validate the simple average of high-resolution measurements such as the PR observations to the (coarser) model resolution. The upscaling/downscaling technique, developed by [Perica and Foufoula-Georgiou \(1996a\)](#) is based on wavelet decomposition and provides insights on the scale invariance properties of the rainfall fluctuations at different scales. Its natural application is for downscaling of rainfall model fields from coarser to finer resolution. Here it is applied in the “opposite” direction, to reconstruct an average from high resolution measurements. Comparisons showed that a simple average can be used with a good degree of confidence in the estimation of model first guess and 1D–Var retrieval biases.

**Acknowledgement** Many thanks to Dr V. Venugopal for kindly providing the downscaling software and assistance in its use; thanks also to Dr E. Foufoula–Georgiou, who pioneered work in rainfall statistical downscaling, for her advice. The TRMM/PR data relative to the seventeen tropical cyclones were downloaded from [www.eorc.nasda.go.jp/TRMM/tropical](http://www.eorc.nasda.go.jp/TRMM/tropical). Thanks to the curator of this website for an excellent job in keeping this page updated and easily accessible. This research was performed under CloudSat NASA grant NAS5–99237 and European Space Agency project EGPM (#3-10600/02/NL/GS).

## References

- Bauer, P.: 2001, Including a melting layer in microwave radiative transfer simulation for clouds. *Atmos. Research*, **57**, 9–30.
- 2002, Microwave radiative transfer modelling in clouds and precipitation. Part I: Model description. Technical report, satellite Application Facility for Numerical Weather Prediction, NWPSAF-EC-TR-005, version 1.0.
- Bauer, P., P. Amayenc, C. D. Kummerow, and E. A. Smith: 2001, Over-ocean rainfall retrieval from multi-sensor data of the Tropical Rainfall Measuring Mission (TRMM). Part II: Algorithm implementation. *J. Ocean. Atmos. Tech.*, **18**, 1838–1855.

- Bauer, P. and P. Schluessel: 1993, Rainfall, total water, ice water, and water vapor over sea from polarized microwave simulations and special sensor microwave/imager data. *J. Geophys. Res.*, **98**, 20737–20759.
- Conner, M. D. and G. W. Petty: 1998, Validation and intercomparison of SSM/I rain-rate retrieval methods over the Continental United States. *J. Appl. Meteor.*, **37**, 679–700.
- Courtier, P., J.-N. Thépaut, and A. Hollingsworth: 1994, A strategy for operational implementation of 4D-Var, using an incremental approach. *Q. J. R. Meteor. Soc.*, **120**, 1367–1387.
- Cunning, J. B.: 1986, The Oklahoma–Kansas Preliminary Regional Experiment for STORM–Central. *Bull. Am. Meteorol. Soc.*, **67**, 1478–1486.
- Harris, D. and E. Foufoula-Georgiou: 2001, Subgrid variability and stochastic down scaling of modeled clouds: Effects on radiative tranfer computation for rainfall retrievals. *J. Geophys. Res.*, **106**, 10,349–10,362.
- Harris, D., E. Foufoula-Georgiou, and C. Kummerow: 2003, Effects of underrepresented hydrometeor variability and partial beam filling on microwave brightness temperature for rainfall retrieval. *J. Geophys. Res.*, **108**, 8380 doi:10.1029/2001JD001144.
- Iguchi, T., T. Kozu, R. Meneghini, J. Awaka, and K. Okamoto: 2000, Rain profiling algorithm for TRMM Precipitation Radar data. *J. Appl. Meteor.*, **39**, 2038–2052.
- Jakob, C., R. Pincus, C. Hannay, and K.-M. Xu: 2003, The use of cloud radar observations for model evaluation: a probabilistic approach. *J. Geophys. Res.*, submitted on January 30, 2003.
- Kozu, T. and T. Iguchi: 2001, A preliminary study of non-uniform beam filling correction for spaceborne radar rainfall measurement. *IEICE TRANS. COMMUN.*, **E79-B**, 763–769.
- Kozu, T., T. Kawanishi, H. Kuroiwa, M. Kojima, K. Oikawa, H. Kumagai, K. Okamoto, M. Okumura, H. Nakatsuka, and K. K. Nishikawa: 2001, Development of Precipitation Radar onboard the Tropical Rainfall Measuring Mission (TRMM) satellite. *IEEE Trans. Geosci. Remote Sensing*, **39**, 102–116.
- Le Marshall, J. F., L. M. Leslie, R. F. Abbey Jr, and L. Qi: 2002, Tropical cyclone track and intensity prediction: The generation and assimilation of high-density, satellite-derived data. *Meteorol. Atmos. Phys.*, **80**, 43–57.
- Locatelli, J. D. and P. V. Hobbs: 1974, Fall speeds and masses of solid precipitation. *J. Geophys. Res.*, **79**, 2185–2197.
- Lopez, P. and E. Moreau: 2004, A convection scheme for data assimilation: Description and initial tests. Technical report, ECMWF Technical Memorandum No. 411. Accepted for publication in *Q. J. R. Meteorol. Soc.*
- Marécal, V. and J.-F. Mahfouf: 2000, Variational retrieval of temperature and humidity profiles from TRMM precipitation data. *Mon. Weather Rev.*, **128**, 3853–3866.
- Marshall, J. S. and W. M. Palmer: 1948, The distribution of raindrops with size. *J. Meteor.*, **5**, 165–166.
- Moreau, E., P. Bauer, and F. Chevallier: 2002, Microwave radiative transfer modelling in clouds and precipitation. Part II: Model evaluation. Technical report, satellite Application Facility for Numerical Weather Prediction, NWPSAF-EC-TR-005, version 1.0.
- Moreau, E., P. Lopez, P. Bauer, A. M. Tompkins, M. Janisková, and F. Chevallier: 2004, Variational retrieval of temperature and humidity profiles using rain rates versus microwave brightness temperatures. *Q. J. R. Meteorol. Soc.*, **130**, 827–852.



- Perica, S. and E. Foufoula-Georgiou: 1996a, Linkage of scaling and thermodynamic parameters of rainfall: results from midlatitude mesoscale convective systems. *J. Geophys. Res.*, **101**, 7431–7448.
- 1996b, Model for multiscale disaggregation of spatial rainfall based on coupling meteorological and scaling descriptions. *J. Geophys. Res.*, **101**, 26,347–26,361.
- Pincus, R. and S. A. Klein: 2001, Unresolved spatial variability and microphysical process rates in large-scale models. *J. Geophys. Res.*, **105**, 27,059–27,065.
- Simpson, J., C. Kummerow, W.-K. Tao, and R. F. Adler: 1996, On the Tropical Rainfall Measuring Mission (TRMM). *Meteorol. Atmos. Phys.*, **60**, 19–36.
- Stephens, G. L., S.-C. Tsay, P. W. Stackhouse, and P. J. Flatau: 1990, The relevance of the microphysical and radiative properties of cirrus clouds to climate and climatic feedback. *J. Atmos. Sci.*, **47**, 1742–1753.
- Tompkins, A. M. and M. Janisková: 2004, A cloud scheme for data assimilation: Description and initial tests. *Q. J. R. Meteorol. Soc.*, **130**, 2495–2517.
- Tustison, B., E. Foufoula-Georgiou, and D. Harris: 2003, Scale-recursive estimation for multisensor quantitative precipitation forecast verification: A preliminary assessment. *J. Geophys. Res.*, **108**, 8377 10.1029/2001JD001073.
- Tustison, B., D. Harris, and E. Foufoula-Georgiou: 2001, Scale issues in verification of precipitation forecasts. *J. Geophys. Res.*, **106**, 11,775–11,784.
- Webster, P. J.: 1994, The role of hydrological processes in ocean–atmosphere interactions. *Rev. Geophys.*, **32**, 427–476.
- Wilks, D. S.: 1995, *Statistical methods in the atmospheric sciences*. Academic Press.